Colour–magnitude relations and spectral line strengths in the Coma cluster

A. I. Terlevich,[1] Harald Kuntschner,[2] R. G. Bower,[2] N. Caldwell[3] and R. M. Sharples[2]

[1]*University of Birmingham, Edgbaston, Birmingham B15 2TT*
[2]*University of Durham, South Road, Durham DH1 3LE*
[3]*F.L. Whipple Observatory, Smithsonian Institution, PO Box 97, Amado, AZ 85645, USA*

ABSTRACT

We use the C_24668, Fe4383, $H\gamma_A$ and $H\delta_A$ spectral absorption line indices, together with *U*- and *V*-band photometry of 101 galaxies in the Coma cluster, to investigate how mean age and metal abundance correlate with galaxy luminosity. In particular, we use the line index measurements to address the origin of the colour–magnitude relation (CMR). We find that the CMR in Coma is driven primarily by a luminosity–metallicity correlation. We additionally show evidence for a relation between age and luminosity, in the direction predicted by the semi-analytic hierarchical clustering models of Kauffmann & Charlot, but this is only present in the C_24668 index models, and could be an effect of the lack of non-solar abundance ratios in the Worthey models used.

By comparing deviations from the CMR with deviations in absorption index from analogous 'index–magnitude' relations, we find that colour deviations bluewards of the mean relation are strongly correlated with the hydrogen Balmer line series absorption. We show that the properties of these blue galaxies are consistent with the presence of a young stellar population in the galaxies, rather than with a reduced metallicity.

Key words: galaxies: abundances – galaxies: clusters: individual: Coma – galaxies: elliptical and lenticular, cD – galaxies: formation – galaxies: starburst.

1 INTRODUCTION

It has been long understood that the colours of early-type galaxies are governed primarily by the effects of age and metallicity, which, when increased, cause the spectral energy distribution (SED) to become redder (Renzini & Buzzoni 1986; Buzzoni, Gariboldi & Mantegazza 1992; Buzzoni, Chincarini & Molinari 1992; Worthey 1994; Charlot & Silk 1994). In his '3/2' law ($\Delta \log(t) \sim \frac{3}{2} \Delta[\mathrm{Fe/H}]$), Worthey (1994) demonstrated how age and metallicity have a degenerate effect on galaxy colours. The colour–magnitude relation (CMR), in which the colours of early–type galaxies become progressively redder with increasing luminosity, and hence increasing mass of the galaxy (Visvanathan & Sandage 1977) is seen in the cores of rich clusters, in groups, and even seems to be present in field ellipticals (Larson, Tinsley & Caldwell 1980). Traditionally, the slope seen in the CMR has been attributed to a mass–metallicity sequence (Dressler 1984; Vader 1986), with the massive galaxies being more metal rich, and thus redder, than the less massive ones. This tendency can naturally be explained by a supernova–driven wind model (Larson 1974; Arimoto & Yoshii 1987), in which more massive

galaxies can retain their supernova ejecta for longer than can smaller galaxies, thus being able to process a larger fraction of their gas before it is expelled from the galaxy. Given the degeneracy between the metallicity and age of a stellar population in its broad-band colours, it is also possible that the CMR is an age-driven sequence, with the smaller galaxies being bluer owing to a lower mean age of their stellar populations. An age-dependent CMR however neither preserves its slope, nor its magnitude range with time (Kodama 1997; Kodama & Arimoto 1997). Studies of the CMR in high-redshift clusters find a ridge-line slope comparable to that of the local clusters; furthermore, there is no sign of a change in the range of magnitude over which the CMR may be traced (Ellis et al. 1997; Stanford, Eisenhardt & Dickinson 1998). This makes an age-dependent CMR in clusters highly unlikely. Given this metallicity driven interpretation of the CMR, its low levels of scatter in cluster cores implies that the galaxies are made up from uniformly old stellar populations (Bower, Lucey & Ellis 1992; Bower, Kodama & Terlevich 1998). Even small variations in the ages of the galaxies would lead to unacceptable levels of scatter in young stellar populations, whereas old stellar populations have a much smaller age dependency in their colours.

On closer inspection however, this picture runs into some

★ E-mail: ale@star.sr.bham.ac.uk

problems. At high redshifts, the fraction of blue galaxies in many of the clusters increases (Butcher & Oemler 1978; Butcher & Oemler 1984). Couch & Sharples (1987) spectroscopically investigated the galaxies in some of these 'Butcher–Oemler' clusters. They split their sample into blue and red galaxies depending on whether they lie on the cluster CMR or not, and associate the increased fraction of blue galaxies with either ongoing or recent star formation. They also found that 11 out of their 73 red galaxies showed enhanced Balmer absorption lines, indicative of recent bursts of star formation, although it is possible that these red Hδ strong galaxies can be formed by the truncation of star formation in spiral galaxies (Barbaro & Poggianti 1997).

Spectroscopic studies of early-type galaxies in local rich clusters (Caldwell et al. 1993, hereafter C93; Caldwell et al. 1996) have shown that these low-z clusters also contain a population of galaxies with abnormal spectra. They exhibit enhanced Balmer absorption lines, indicative of recent star formation, but with too weak an [O II] line to be classified simply as spiral galaxies. They note the similarity of some of these spectra with the 'red' Hδ-strong galaxies of Couch & Sharples (1987), and find that of the galaxies associated with the dynamically separate group of galaxies centred on NGC 4839 in the south-west of the Coma cluster (Baier 1984; Escalera, Slezak & Mazure 1992; Colless & Dunn 1996), about 1/3 have abnormal spectra.

These spectroscopic studies of local and distant clusters have shown there to be a population of galaxies which, although they appear photometrically old, have been forming significant quantities of stars in their recent past.

In an effort to disentangle age and metallicity effects on stellar populations, Worthey (1994) (also Worthey & Ottaviani 1997) developed a series of stellar population spectral synthesis models, to show the dependence on age and metallicity of spectral features such as the Balmer lines and various metal lines. In a study of a magnitude-limited sample ($M_B < -17$) of early-type galaxies in the Fornax cluster, Kuntschner & Davies (1998) used these models to show that, as predicted by the high-z studies, the elliptical galaxies are indeed uniformly old, and span a range in metallicities. They also showed that the majority of the (luminosity weighted) young galaxies in the cluster were low-luminosity lenticular systems. However, earlier studies of mainly field early-type galaxies (González 1993; Trager 1997) show just the opposite, with these galaxies seeming to have a uniform metallicity and a range of ages, yet still forming a well-defined CMR. This points to the possibility of an environmental dependence of the CMR, or maybe two completely different mechanisms operating in cluster and field environments, conspiring to produce similar CMRs.

In this paper we will look at spectral line indices and deviations from the CMR in the Coma cluster, using both the Worthey (1994) and Worthey & Ottaviani (1997) spectro-photometric evolution models. We use the high-precision photometry of the Coma cluster presented in Terlevich et al. (in preparation, hereafter T99, also Terlevich 1998) and the spectra of Coma cluster galaxies from C93. The selection of galaxies and the spectroscopic and photometric measurements are outlined in Section 2. Our principle goal is to investigate whether the CMR in Coma is principally driven by age or metallicity and to determine the cause of deviations from the CMR in individual galaxies. Our analysis is presented in Section 3, followed by a summary of our conclusions in Section 4.

Table 1. The morphological types for the C93 galaxies (Andreon et al. 1996; Andreon et al. 1997), split into the three coarse bins of spiral/late-type, S0 and elliptical (see text).

Morphological type	Number of galaxies
No morphology	31
Spiral/late-type	12
S0	47
E	11
All types	101

2 THE DATA

The overall aim of this paper requires us to combine accurate photometry with precise line-index measurements. The aperture photometry of T99 covers an area of the Coma cluster that is well matched to the spectroscopic survey of C93. As a result, we are able to compare the spectroscopic and broad-band colours of 101 galaxies drawn from within $50'$ of the cluster centre.[1] Below we describe the selection of the spectroscopic catalogue, the spectroscopic determination of line-strength indices, and the matching photometric measurements.

2.1 Sample selection

C93 selected their sample from the extensive galaxy catalogue of Godwin, Metcalfe & Peach (1983) (hereafter GMP). The parent catalogue is drawn from a 2.6 deg^2 field, centred on the Coma cluster, and is considered complete to $B = 20$, corresponding to $M_B < -14.2$.[2] C93 used two criteria to select early-type galaxies from the GMP sample. First they fitted the GMP $(B, B - V)$[3] colour magnitude relation and selected all galaxies whose colours lay within ± 0.15 mag of the fit. Secondly, they obtained independent morphologies using KPNO 4-m and Palomar Sky Survey plates. Using these morphologies, and those of Dressler (1980) they removed morphologically late-type systems from the list, and added some (~ 25) morphologically early-type galaxies which had failed to be included after the colour cut. Finally they rejected all galaxies brighter than $B = 14.3$, as high-velocity dispersion in these more massive galaxies would make their spectroscopic analysis of weak absorption lines impossible. We have further trimmed their sample of 137 galaxies by rejecting the ones which had the lowest signal-to-noise ratio and the emission-line galaxies, leaving us with a total of 101 galaxies.

Table 1 shows the distribution of Andreon et al. (1996) and Andreon, Davoust & Poulain (1997) morphological types for the C93 galaxies. Immediately obvious is the fact that 12 of the Caldwell early-type galaxies are in fact late-types according to Andreon et al. (1996). Although only one of these turns out to lie more than two standard deviations blueward of the $U - V$ CMR ridge line (see Fig. 1 and Section 3.1). It must be noted, however,

---

[1] An ASCII table of the galaxy colours and line indices is available on request via e-mail from A. I. Terlevich (also available as Supplementary Material in the electronic version of MNRAS).

[2] We take the recessional velocity of the Coma cluster to be ~ 6800 km s^{-1} (Colless & Dunn 1996), and assume $H_0 = 100$ km s^{-1} Mpc^{-1}, which gives a distance modulus of $(m - M) = 34.2$.

[3] C93 converted the GMP $(b - r)$ colours to $(B - V)$ colours using galaxies in common with the compilation of Burstein et al. (1987).
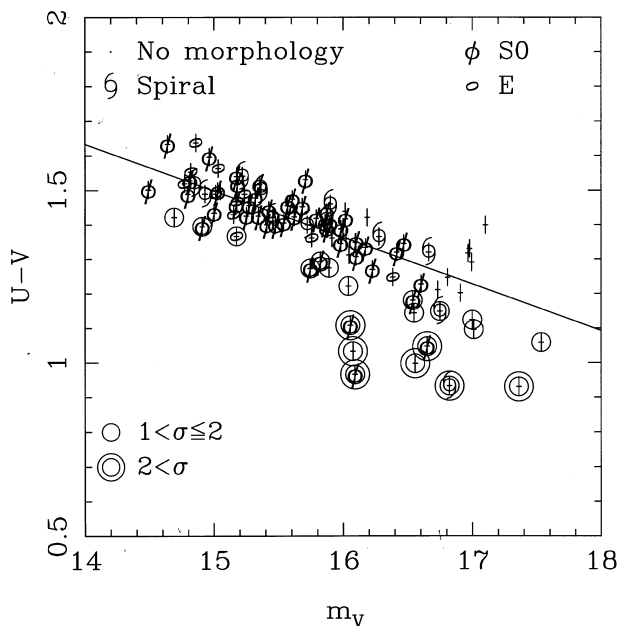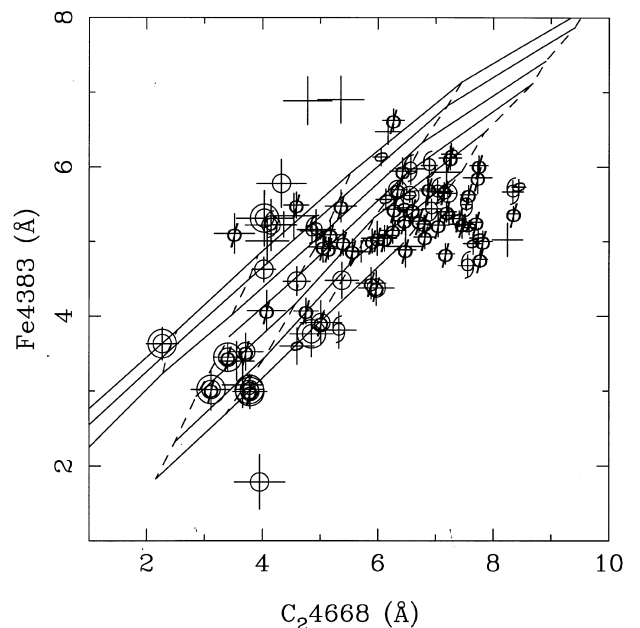
Figure 1. The $U - V$ colour–magnitude relation for the subsample of 101 Coma galaxies for which we have appropriate signal-to-noise ratio spectra, both colours and magnitudes are taken using 8.8-arcsec diameter apertures. The standard deviation about the best fit (solid line) is 0.07 ± 0.01 mag. The symbols are coded by the morphological type of each galaxy. Galaxies which lie between 1 and 2 standard deviations blueward of the CMR best fit have an additional circle drawn around the graph marker. Galaxies which lie more than 2 standard deviations blueward of the CMR best fit have two extra circles drawn about their graph markers. The same symbol scheme is used for the galaxies in all the figures throughout this paper.

Figure 2. The index–index relation between the two metal line indices used in this paper for the sample of Coma galaxies. A grid of single age stellar population models from Worthey (1994) is overplotted. Solid lines connect points of equal age; dashed lines connect points of equal metal abundance. The figure shows that for absorption strengths of $C_2 4668 > 6$ Å, the models do not match the parameter space occupied by the observations very well. This is most simply interpreted as an 'overabundance' of $C_2 4668$ compared to Fe. The symbols, which are defined in Fig. 1, are coded by galaxy morphology, and residual from the CMR.

that up-to-date morphological information for many of the fainter galaxies in the sample is not available, and that this is where most of the blue galaxies reside. Nevertheless, only three out of the seven bluest galaxies have no determined morphologies.

2.2 Spectroscopy

The C93 spectra were all taken on the KPNO 4-m telescope, using the HYDRA multi-fibre positioner. They have a spectral resolution of 3.8 Å (FWHM), and the fibre aperture was 2 arcsec in diameter. In order to compare the spectra with Worthey stellar population models (Worthey 1994; Worthey & Ottaviani 1997), the spectra were re-sampled to the Lick/IDS resolution by convolution with a Gaussian of wavelength-dependent width. Because the C93 data does not include any observations of stars in common with the Lick/IDS, the prescription used was that of Kuntschner (1998) who used it to correct his 4.1 Å (FWHM) resolution Fornax data to the Lick/IDS system. Both the Kuntschner (1998) and the C93 spectra cover a similar wavelength range, and unlike the Lick/IDS spectra, whose spectral resolution degrades notably towards the blue (see fig. 7 of Worthey & Ottaviani 1997) they have a constant spectral resolution over their entire wavelength range. The errors on the indices were estimated from the photon noise of the spectra, and do not take any systematic errors into account. The most likely source of systematic error is the re-sampling of the data on to the Lick/IDS system. Nevertheless, the possible systematic errors will have little effect on the relative comparisons made in this paper. We note that in addition, our Poisson error evaluation probably

underestimates the true error because response variations from fibre to fibre will introduce extra scatter.

The final step necessary to place the line indices into the Lick/IDS system is to correct the galaxy spectra for velocity dispersion. Velocity dispersion corrections for individual line indices were taken from Kuntschner (1998), who calculated them by artificially broadening stellar spectra (e.g. Davies, Sadler & Peletier 1993). The C93 spectra are not of sufficient resolution and signal-to-noise ratio to measure accurate central velocity dispersions for our galaxies, so instead we construct a 'Faber–Jackson' relation (Faber & Jackson 1976) between our V-band 8.8-arcsec diameter aperture magnitudes m_V (see Section 2.3), and the velocity dispersions (σ) of Lucey et al. (1997). A biweight fit (cf. Section 2.3) gives a relation of

$$\log_{10}(\sigma) = (5.6 \pm 0.6) - (0.22 \pm 0.01) \times m_V \qquad (1)$$

(with 1σ bootstrap errors). We used this relation to find values of σ for those galaxies in the C93 sample which were not present in the Lucey et al. (1997) data.

We use the $H\gamma_A$ and $H\delta_A$ Balmer line indices (Worthey & Ottaviani 1997) as the predominantly age sensitive spectral features. While $H\beta$ is more sensitive to age, it is also more affected by nebular emission, which can rapidly fill the absorption feature (González 1993), so is not used. Higher order Balmer lines are less sensitive to emission from ionised gas (Osterbrock 1989), making an accurate measurement of the true stellar absorption easier. In order to increase the signal to noise, we have used $H\delta_A + H\gamma_A$ in the final analysis. The $C_2 4668$ feature is identified by Worthey (1994) as a particularly sensitive metallicity feature.

Table 2. Results of regression analysis with 1σ bootstrap errors for the line indices and colour versus *V*-band magnitude (see Figs 1 and 5).

Index	Intercept	Slope	Scatter
$U - V$	3.5 ± 0.7 mag	-0.14 ± 0.01	0.07 mag
$C_2 4668$	28.9 ± 3.7 Å	-1.45 ± 0.06 Å mag^{-1}	1.05 Å
Fe4383	7.4 ± 8.6 Å	-0.14 ± 0.07 Å mag^{-1}	0.70 Å
$H\delta_A + H\gamma_A$	-18.4 ± 9.3 Å	0.75 ± 0.12 Å mag^{-1}	1.44 Å

However it is possible that it suffers from over abundance problems in the larger, higher metallicity systems (Kuntschner 1998). Fig. 2 shows the relation between $C_2 4668$ and Fe4383 for the Coma galaxies, overplotted are the theoretical relation from Worthey (1994) models. Above a value of ~ 6 Å, the measured $C_2 4668$ index values deviate from the region predicted by the models. A similar effect is seen by Kuntschner (1998) for early-type galaxies in the Fornax cluster. However in our data, the Fe4383 index has poorer signal-to-noise ratio than the $C_2 4668$ index, so we will use both, noting the discrepancy for the high metallicity galaxies.

2.3   The photometry

It is important to get as good a match as possible between the photometric and spectroscopic apertures, so that both are measuring the same part of the galaxy. In the case, for instance, of localised bursts of star formation occurring in the galaxy nucleus, the large photometric aperture and the small spectroscopic one, could well both be measuring different mixes of stellar populations.

In order to match the 2-arcsec diameter of the HYDRA fibres used for the spectra as best as possible, we use the 8.8-arcsec diameter photometry from T99. The use of smaller metric apertures was not possible owing to the increased effects of variations in seeing conditions during the observations. The T99 catalogue covers an area of 3360 arcmin^2 to a depth of $V_{13} = 20$ mag (ie., *V*-band magnitude within a $13''$ diameter aperture) giving Johnson *U*- and *V*-band magnitudes for ~ 1400 extended objects. The RMS internal scatter in the photometry is 0.014 mag in V_{13}, and 0.026 mag in U_{13} for $V_{13} < 17$ mag.

Throughout this paper we use the biweight minimizing technique, described in T99 (see also Beers, Flynn & Gebhardt 1990) to fit linear relations to the data. It was used for its resistance to outlying data points, and its robustness against non-Gaussian noise distributions. We derive the residuals of indices and colours from a mean index or colour–magnitude relation by the following equation:

$$\Delta(X) = X - (b_X \times m_V + c_X) \qquad (2)$$

where X is a line index ($C_2 4886$, Fe4383 or $H\delta_A + H\gamma_A$), or $(U - V)$ colour, b_X and c_X are the slope and intercept of the best-fitting relation (see Table (2)), and m_V is the *V* magnitude.

## 3   IMPLICATIONS FOR STAR FORMATION HISTORIES AND THE ORIGIN OF THE CMR

3.1   The colour–magnitude relation

Given the selection criterion of C93, we should expect the CMR to be prominent in our $(V, U - V)$ data-set. As can be seen in Fig. 1, the biweight scatter is indeed small: $\sigma = 0.07 \pm 0.01$ mag. Somewhat more surprising is the significant number of galaxies

deviating blueward of the mean relation towards the faint end. The effect is not seen in the $(B, B - V)$ relation of C93 (see fig. 1 in C93), presumably owing to the lower sensitivity of $B - R$ colour to age, combined with their larger photometric errors. In order to trace the position of these relatively faint and blue galaxies in the subsequent figures, we adopt a common labelling convention throughout the paper. The symbols reflect the morphologies taken from Andreon et al. (1996) and Andreon et al. (1997), as defined by the key in Fig. 1. The number or rings plotted around each symbol indicates its deviation from the best-fitting CMR. Points without rings lie either redward of the colour-magnitude relation, or are within 1σ of it. Points with only one ring lie between 1σ and 2σ blueward of the relation, and points with two rings lie more than 2σ blueward of the relation. Unless otherwise stated, when we refer to 'blue' galaxies we are referring to the objects plotted with *at least* one ring, and 'red' galaxies are the objects plotted with no rings.

3.2   Line index diagrams

We have used the Fe4383, $C_2 4668$ and $H\delta_A + H\gamma_A$ indices to place the galaxies on Worthey's age/metallicity diagnostic diagrams (Figs 3 and 4). In these figures, solid lines trace loci of constant age, from 1.5 to 17 Gyr (positive to negative $H\delta_A + H\gamma_A$ values). Dashed lines trace loci of constant [Fe/H] from -2.0 to $+0.5$ (lowest to highest metal line strength). Note that small systematic offsets ($\lesssim 0.5$ Å) between the model and the observed index systems may well be present. We must stress that these models represent single stellar population (SSP) systems, whereas our galaxies contain a mixture of stellar populations of different ages and metallicities. The indices we measure are therefore a luminosity weighted mean index of all of the different populations
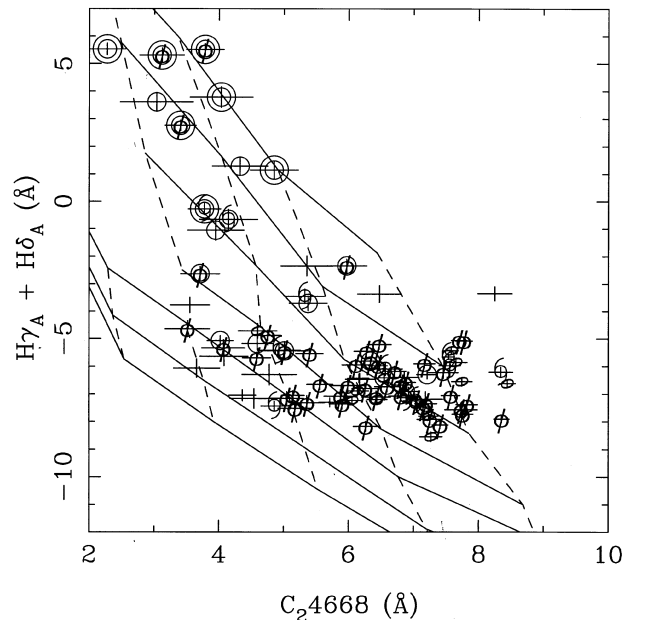
Figure 3. The distribution of galaxies in the $(C_2 4668, H\delta_A + H\gamma_A)$ plane, with a model grid of single stellar population models (Worthey 1994; Worthey & Ottaviani 1997). Solid lines trace loci of constant age (1.5, 2, 3, 5, 8, 12 and 17 Gyr from positive to negative $H\delta_A + H\gamma_A$ values). Dashed lines trace loci of constant [Fe/H] (-0.5, -0.25, 0.0, 0.25 and 0.5 from lowest to highest metal line strength). The different symbols correspond to the morphology of each galaxy, and its offset from the colour–magnitude relation as defined in Fig. 1.
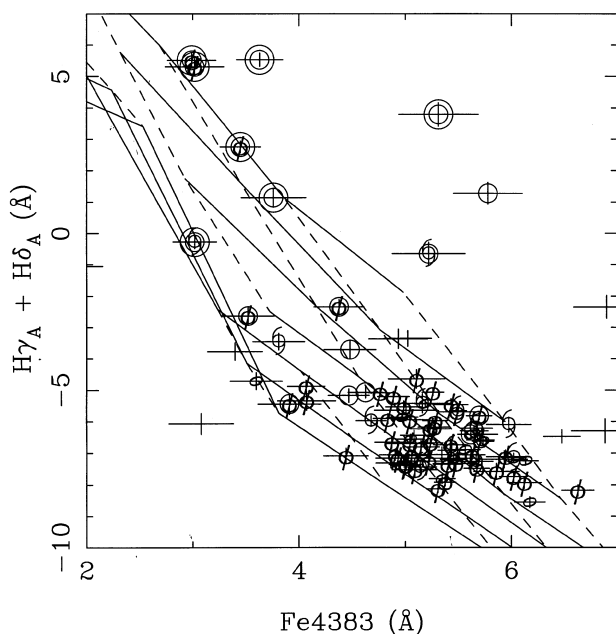
Figure 4. The distribution of galaxies in the (Fe4383, $H\delta_A + H\gamma_A$) plane, with a model grid of single stellar population models (Worthey 1994; Worthey & Ottaviani 1997). Solid lines trace loci of constant age, from 1.5 to 17 Gyr. Dashed lines trace loci of constant [Fe/H] from -0.5 to 0.5. The different symbols correspond to the morphology of each galaxy, and its offset from the colour–magnitude relation as defined in Fig. 1.

present in each galaxy, and the higher luminosity of a young stellar population can mean that even the addition of a small percentage (by mass) of young stars into an old galaxy, can severely affect its overall 'age'. For example, if one adds a 10 per cent (mass), $1\,\mathrm{Gyr}$, [Fe/H] = +0.5 population, to an $18\,\mathrm{Gyr}$, [Fe/H] = 0 population, the resultant stellar population would have the same line strengths as a $2\,\mathrm{Gyr}$, [Fe/H] = +0.25 SSP (Trager 1997). In this paper, when we refer to a galaxy as 'young', we are referring only to its luminosity weighted mean age.

As we would expect, the blue and red galaxies occupy different areas of the line index diagrams. The blue galaxies which deviate by more than 2σ from the CM relation (Fig. 1) tend to populate the low-age portion of the grid. The trend is common to the lower colour deviation galaxies as well: only six out of the 20 blue galaxies lie on the same part of the Worthey grid populated by the red galaxies. Both figures imply a low age for the blue galaxies (an effect driven mainly by the $H\delta_A + H\gamma_A$ index); however they seem to indicate different trends for the the red galaxies which make up the ridge of the CMR. In Fig. 3 red galaxies span a range both in metallicity and in age, seeming to indicate a far from simple formation scenario, especially as the more massive galaxies appear to have the lower ages. We must remember however, that the model grids at these high metallicities are far from secure. In particular, we have already noted the over-abundance problem in the models for galaxies with $C_24668 > 6\,\text{Å}$ in Section 2.2. If we ignore these galaxies, the span in age and metallicity of the red galaxies is reduced.

Fe4383 does not suffer from the same overabundance effects as C_24668, however it also has more of an age dependence, producing slightly more degenerate model grids. In addition, the measurements have larger relative errors. In Fig. 4, we can see again that the blue galaxies have younger ages than do the red

ones, however they no longer exclusively populate the low-metallicity portion of the grid. Some of the galaxies are in parts of the plot completely outside the parameter space covered by the model grid, although these are the galaxies with the largest error bars in the Fe4383 data. The red galaxies have a lower spread in metallicity, and do not follow the same trend in age as in Fig. 3, however, owing to the increased scatter in the Fe4383 data, and the increased degeneracy in the model grid, it is still not possible to say that they follow a single age population model line. This may simply be due to the lower signal to noise of the Fe4383 index.

It is worth noting that there is a morphological segregation in Figs 3 and 4. In both figures all of the elliptical galaxies populate the old portion of the model grids, while the S0s and late type galaxies are spread over the grid. This seems to indicate there are both old and young S0 and late type galaxies, but only old ellipticals (Kuntschner & Davies 1998; Kuntschner 1998; Mehlert et al. 1998). The overall effect seems to be connected with galaxy luminosity, with the lower luminosity galaxies having more varied star formation histories.

3.3 Colour residuals versus line-strength residuals

In Section 3.2, we showed that the blue galaxies which deviate from the mean CMR have younger luminosity weighted ages than do the red galaxies. In this section we shall further investigate the correlation between colour offsets from the CMR, and analogous offsets from spectral index versus magnitude relations (IMR) (Fig. 5).

We define the mean IMR in the same way as we defined the mean CMR, by using the biweight estimator (see Section 2.3) to get a linear relation between the spectral line strength and luminosity of a galaxy. We list the results of the fits in Table 2, and they are shown as the solid lines in Fig. 5. The residuals from the mean IMR are defined using equation (2).

Fig. 5 and Table 2, show that we can define IMRs for all of our spectral indices. The C_24668 relation (Fig. 5a) shows the best correlation, which fits in with the interpretation of the CMR as a metallicity sequence, since C_24668 is the most metallicity sensitive of our three spectral indices (Worthey 1994). The $H\delta_A + H\gamma_A$ relation (Fig. 5c) also has an obvious IMR. Unlike the C_24668 IMR, the red galaxies make up a relation of increasing $H\delta_A + H\gamma_A$ with decreasing luminosity, while most of the blue galaxies are deviant from the relation.

The Fe4383 IMR (Fig. 5b), like the $H\delta_A + H\gamma_A$ IMR, shows increased scatter from the blue galaxies. To demonstrate the effectiveness of the biweight minimisation fit, we show some examples of different types of fit to the data. The solid line is the biweight scatter minimization fit to all the data. The dashed line is the biweight fit to only the red CMR galaxies, the dot–dash line shows the biweight fit to galaxies with $m_V < 16$, and the dotted line shows the fit to all the data, using a method which bisects the ordinary least squares fits made by minimizing the X and the Y residuals (Isobe et al. 1990; Feigelson & Babu 1992). The biweight fit, and the least-squares fit to only the red galaxies are almost identical. As is the case with the $H\delta_A + H\gamma_A$ relation, most of the deviation comes from the blue galaxies, so we again take the biweight fit as the definition of the mean population. It should be noted that there is a much larger bootstrap uncertainty in the slope of the Fe4383 IMR than with any of the others (see Table 2), making the existence of a non-zero slope to the relation only a 2σ result.
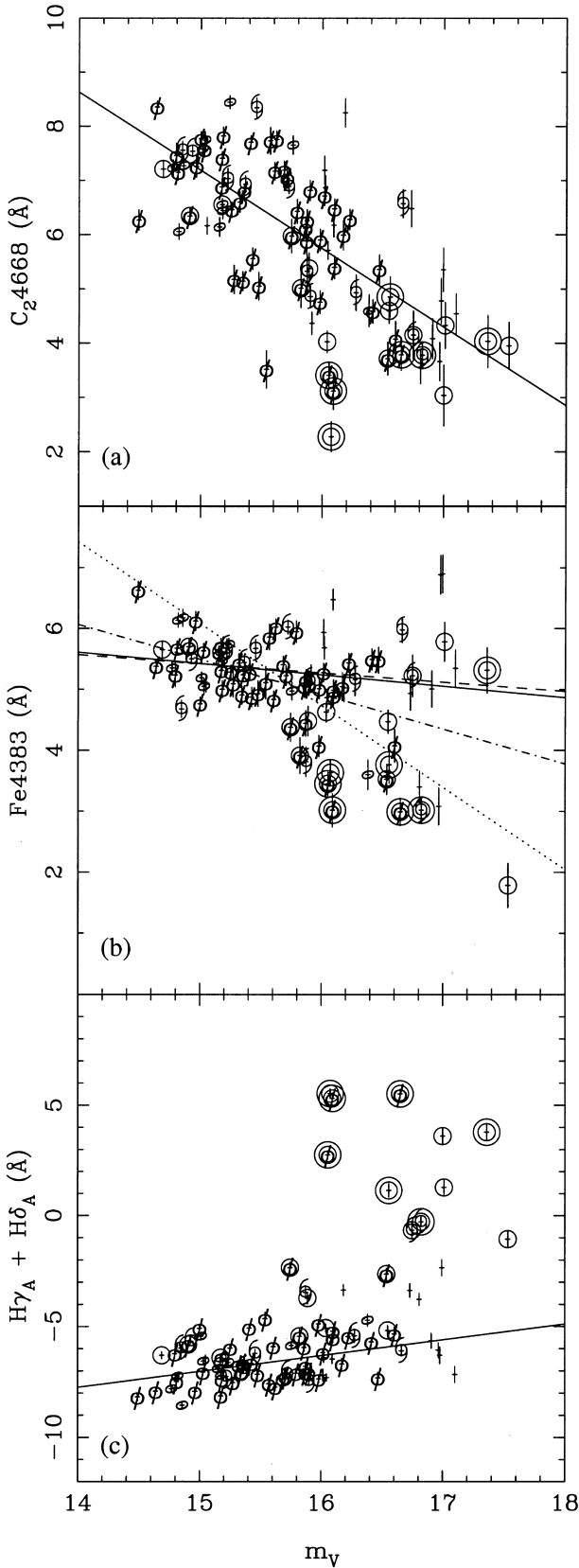
Out of the three indices we investigate, C_24668 is the most sensitive to metallicity, and indeed shows the greatest correlation with galaxy luminosity. This diagram agrees with the standard paradigm of a metal abundance driven CMR. The poorer correlation of Fe4383 is initially surprising, but seems to reflect the lower metal abundance sensitivity of the Fe4383 index relative to C_24668, a difference that is enhanced by the so-called 'over abundance' effect (cf. Fig. 2). This leads to the interesting possibility that the CMR is in fact driven by a correlation between luminosity and metal overabundance, however further investigation of this possibility would require improved spectra, and is beyond the scope of the present work. Finally, we note that models of the Fe4383 index have more of a dependence on age than C_24668; thus an age gradient along the CMR (in the sense of fainter galaxies having lower ages) would tend to steepen the slope. This effect is seen only in the position of the blue galaxies in Fig. 5(b).

We now investigate how deviations from the CMR correlate with deviations from the IMRs. We show the correlations in Fig. 6. To aid the eye, we show the $\pm 1\sigma$ deviations from the CMR and IMRs as dashed horizontal and vertical lines. The dotted line in panel (c) shows the $+3\sigma$ scatter in the $H\delta_A + H\gamma_A$ relation. We have used the Worthey (1994), Worthey & Ottaviani (1997) models to show how changes in age (solid arrow) and metallicity (dotted arrow) would affect galaxies in the CMR/IMR plot. The age arrow was calculated by adding a 15 per cent (by mass) population of 1 Gyr old stars with solar metallicity, to an 8 Gyr old population with solar metallicity. The metallicity arrow was calculated by changing the metallicity of an 8 Gyr old population from $[Fe/H] = 0$ to $[Fe/H] = -0.5$. These arrows can be thought of as vectors, in that increasing the size of the post-starburst population, or decreasing the metallicity of the population further, tends to increase the length of the arrows, without significantly changing their direction. Note however that if a galaxy were undergoing a starburst at the time of observation, it would have Balmer lines (Fig. 6c) in emission, and would therefore have negative $\Delta(H\delta_A + H\gamma_A)$, but it would still posses blue colours (negative $\Delta(U - V)$). This emission quickly fades and turns into absorption, and after ~ 1 Gyr, the galaxies indeed roughly follow the vector shown in Fig. 6(c).

Fig. 6(a) shows deviations from the C_24668 IMR. Only three of the $\Delta(U - V) < -2\sigma$ (double-ringed) galaxies have ΔC_24668 values which lie outside the $\pm 1\sigma$ range indicated by the dashed lines, with the other four double-ringed galaxies lying within $\pm 1\sigma$ of the ΔC_24668 distribution. The age (solid) vector, indicates that we would not expect much C_24668 deviation for $\Delta(U - V) = -0.3$, and indeed the majority of the double-ringed blue galaxies lie close to the age vector. The three double-ringed galaxies most deviant in C_24668, do lie closest to the metallicity vector, however given the large range in the ΔC_24668 indices of the 'red' population, they are not inconsistent with the age vector. By contrast, the age and metallicity vectors for the ΔFe4383 relation

Figure 5. The relation between the line indices and *V* magnitude. The solid line in each panel shows the biweight regression fit used to calculate $\Delta(X)$ (see Table 2). The different symbols correspond to the morphology of each galaxy, and its offset from the colour–magnitude relation (see Fig. 1). In panel (b), the dashed line is the biweight scatter minimization fit to only the red galaxies, the dot–dash line shows the biweight scatter minimization fit to galaxies with $m_V < 16$, and the dotted line shows the fit to all the data, using an ordinary least squares bisector method (see main text).
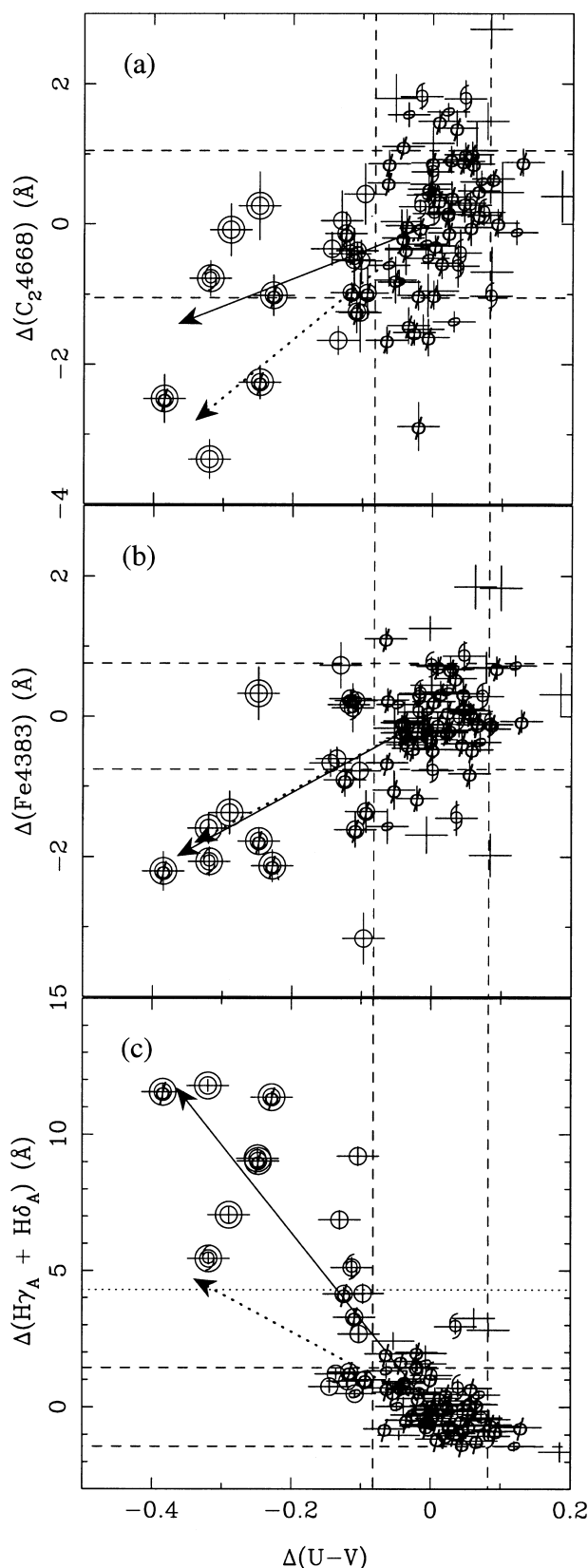
(Fig. 6b) are degenerate, and indeed all but a couple of the blue galaxies lie along these vectors.

The correlation between $\Delta(U - V)$ and $\Delta(H\delta_A + H\gamma_A)$ is the strongest of the three (Fig. 6c). Like Fig. 6(a), there is a significant separation between the age and metallicity vectors, and all but one of the double-ringed blue galaxies lie closer to the age vector than the metallicity one. This includes the three blue galaxies which lie along the metallicity vector in Fig. 6(a). In this case however, the range in the $\Delta(H\delta_A + H\gamma_A)$ indices for the 'red' galaxies is less than the equivalent range of $\Delta C_2 4668$ in Fig. 6(a), and cannot be used to account for the distance of most of the 'blue' galaxies from the metallicity vector. Additionally, all of the double-ringed blue galaxies deviate from the mean $H\delta_A + H\gamma_A$ IMR by more than 3σ (the dotted horizontal line). These effects can only be accounted for by using a younger mean stellar population.

4 IMPLICATIONS

We have shown using both the Fe4383 and the $C_2 4668$ indices, that the 'red' galaxies which make up the colour–magnitude relation in the Coma cluster, span a range of metallicities. Whether this is the sole driving force behind the CMR, or whether there is also a correlation between age and luminosity is more debatable. There is no evidence for an age trend with the age-estimates based on the Fe4383 index, however the $C_2 4668$ models indicate that the more luminous galaxies have lower ages. It could be that the effect is not visible in the Fe4383 models owing to the higher degree of degeneracy in the age and metallicity tracks for this index, but it should be noted that any trend in age comes from the $C_2 4668$ index, at strengths where overabundance effects mean that it is no longer properly predicted by the Worthey models (see Fig. 2 and Vazdekis et al. 1996, 1997). Kuntschner (1998) corrects the $C_2 4668$ index in his Fornax cluster galaxies for such overabundance problems in the models, and shows that much of the age upturn for the bright ellipticals disappears. If the correlation between age and luminosity is real however, it would be in the direction predicted by semi-analytic hierarchical clustering models, which predict that more luminous cluster galaxies should have lower luminosity weighed ages, and higher metallicities, than the less luminous ones (Kauffmann & Charlot 1998). Finally, we note that the sense of this age gradient is such that the CMR cannot be explained by an age variation alone. In contrast, even greater metal abundance variations are required in order to restore the observed slope.

We find that galaxies which deviate bluewards from the CMR, also deviate from the $(H\delta_A + H\gamma_A)$-magnitude and the Fe4383–

Figure 6. The deviation of the galaxies from the mean relation in the three spectral indices ($\Delta(C_2 4668)$ in panel a, $\Delta(Fe4383)$ in panel b, $\Delta(H\delta_A + H\gamma_A)$ in panel c), against their deviation from the mean relation in colour [$\Delta(U - V)$]. The fit to the mean relations are calculated from Figs 1 and 5, and are summarized in table 2. The different symbols correspond to the morphology of each galaxy, and its offset from the colour–magnitude relation (see Fig. 1). The dashed horizontal and vertical lines represent the $\pm 1\sigma$ dispersion in the colours and line strengths. The dotted horizontal line in panel (c) shows the 3σ dispersion in $H\delta_A + H\gamma_A$. The two arrows show how a change in galaxy age (solid arrow) and a change in galaxy metallicity (dotted arrow) would affect a 'normal' galaxy. The age arrow is calculated by adding a 15 per cent population of 1 Gyr old stars to an 8 Gyr old galaxy of the same (solar) metallicity. The metallicity arrow shows how an 8 Gyr old solar metallicity galaxy would move if its metallicity were changed to [Fe/H] $= -0.5$.

magnitude relations, but not the $C_2 4668$–magnitude relation. This is consistent with the colour deviant galaxies having undergone a secondary burst of star formation giving low-luminosity weighted ages, or showing overall lower ages. The interpretation of the CMR as a mainly metallicity sequence, with deviations being caused by age variations seems correct. This allows the CMR to be used to place constraints on the star formation histories of the cluster galaxies, an approached used by many authors (Bower et al. 1992; Stanford et al. 1998; Ellis et al. 1997; Bower et al. 1998).

Despite the attempts of C93 to reject late-type galaxies from their sample, a few still seem to have slipped in. We found that the S0 and late-type galaxies span a range in ages (Kuntschner & Davies 1998; Mehlert et al. 1998), but all elliptical galaxies are old. In addition, it is important to note that the younger galaxies are also lower luminosity galaxies, an effect also seen in the Fornax sample of Kuntschner & Davies (1998), and in low-luminosity ($M_B > 17.5$) Coma S0 galaxies (Caldwell & Rose 1998). Worthey (1997) also found that lower luminosity galaxies have a larger spread of ages. This may indicate that star formation activity is being 'down sized' to lower luminosity objects as the universe becomes older (Cowie et al. 1996) or may simply be an artefact of the greater numbers of lower luminosity galaxies. Of the galaxies which lie on the CMR (the red galaxies) we find no obvious difference between the ages of the early and late types, all of them have old luminosity weighted mean stellar ages. This includes 10 out of the 12 late-type galaxies in the sample, although this result should not be too surprising since their spectroscopic properties will almost certainly be dominated by their bulge.

Finally, we note that the use of CMR-corrected ($U - V$) colours is an efficient way of searching for post-starburst galaxies. The ($B, B - V$) CMR constructed by C93 for these same objects (fig. 8 in C93), shows that them to have a much smaller deviation from the mean population than our $U - V$ colours do. In fact all our very blue objects, which deviate blueward by more than two standard deviations from the CMR colour, have Balmer line strengths that deviate by more than three standard deviations from the red galaxies. If we were to search for the PSB galaxies from scratch, and made a colour cut one standard deviation blueward of the CMR, we would find all of the 3σ deviant Balmer line galaxies, with only a 50 per cent contamination from the 'normal' population.

ACKNOWLEDGMENTS

REFERENCES

Andreon S., Davoust E., Michard R., Nieto J. L., Poulain P., 1996, A&AS, 116, 429
Andreon S., Davoust E., Poulain P., 1997, A&AS, 126, 67
Arimoto N., Yoshii Y., 1987, A&A, 173, 23
Baier F. W., 1984, Astron. Nachr., 305, 175
Barbaro G., Poggianti B. M., 1997, A&A, 324, 490
Beers T. C., Flynn K., Gebhardt K., 1990, AJ, 100, 32
Bower R. G., Lucey J. R., Ellis R. S., 1992, MNRAS, 254, 601
Bower R. G., Kodama T., Terlevich A. I., 1998, MNRAS, 299, 1193
Burstein D., Davies R. L., Dressler A., Faber S. M., Stone R. P. S., Lynden-Bell D., Terlevich R. J., Wegner G., 1987, ApJS, 64, 601
Butcher H., Oemler J. A., 1978, ApJ, 226, 559
Butcher H., Oemler J. A., 1984, ApJ, 285, 426
Buzzoni A., Gariboldi G., Mantegazza L., 1992, AJ, 103, 1814
Buzzoni A., Chincarini G., Molinari E., 1993, ApJ, 410, 499
Caldwell N., Rose J. A., 1998, AJ, 115, 1423
Caldwell N., Rose J. A., Sharples R. M., Ellis R. S., Bower G., 1993, AJ, 106, 473 (C93)
Caldwell N., Rose J. A., Franx M., Leonardi A. J., 1996, AJ, 111, 78
Charlot S., Silk J., 1994, ApJ, 432, 453
Colless M., Dunn A. M., 1996, ApJ, 458, 435
Couch W. J., Sharples R. M., 1987, MNRAS, 229, 423
Cowie L. L., Songaila A., Hu E. M., Cohen J. G., 1996, AJ, 112, 839
Davies R. L., Sadler E. M., Peletier R. F., 1993, MNRAS, 262, 650
Dressler A., 1980, ApJS, 42, 565
Dressler A., 1984, ApJ, 281, 512
Ellis R. S., Smail I., Dressler A., Couch W. J., Oemler J., Augustus ??, Butcher H., Sharples R. M., 1997, ApJ, 483, 582
Escalera E., Slezak E., Mazure A., 1992, A&A, 264, 379
Faber S. M., Jackson R. E., 1976, ApJ, 204, 668
Feigelson E. D., Babu G. J., 1992, ApJ, 397, 55
Godwin J. G., Metcalfe N., Peach J. V., 1983, MNRAS, 202, 113 (GMP)
González J. J., 1993, PhD thesis. Univ. California, Santa Cruz,
Isobe T., Feigelson E. D., Akritas M. G., Babu G. J., 1990, ApJ, 364, 104
Kauffmann G., Charlot S., 1998, MNRAS, 294, 705
Kodama T., 1997, PhD thesis, Institute of Astronomy, Univ.Tokyo,
Kodama T., Arimoto N., 1997, A&A, 320, 41
Kuntschner H., 1998, PhD thesis, Department of Physics, Univ. Durham,
Kuntschner H., Davies R. L., 1998, MNRAS, 295, L29
Larson R. B., 1974, MNRAS, 169, 229
Larson R. B., Tinsley B. M., Caldwell C. N., 1980, ApJ, 237, 692
Lucey J. R., Guzman R., Steel J., Carter D., 1997, MNRAS, 287, 899L
Mehlert D., Bender R., Saglia R. P., Wegner G., 1998, in Mazure A., Casoli F., Durret F., Gerbal D., eds, Untangling Coma Berenices: A New Vision of an Old Cluster. World Scientific, Singapore, p. 107
Osterbrock D. E., 1989, Astrophysics of Gaseous Nebulae and Active Galactic Nuclei. University Science Books, New York
Renzini A., Buzzoni A., 1986, Spectral Evolution of Galaxies. Reidel, Dordrecht, p. 195
Stanford S. A., Eisenhardt P. R., Dickinson M., 1998, ApJ, 492, 461
Terlevich A., 1998, PhD thesis, Department of Physics, Univ. Durham,
Trager S. C., 1997, PhD thesis, Univ. California, Santa Cruz,
Vader J. P., 1986, ApJ, 306, 390
Vazdekis A., Casuso E., Peletier R. F., Beckman J. E., 1996, ApJS, 106, 307
Vazdekis A., Peletier R. F., Beckman J. E., Casuso E., 1997, ApJS, 111, 203
Visvanathan N., Sandage A., 1977, ApJ, 216, 214
Worthey G., 1994, ApJS, 95, 107
Worthey G., Ottaviani D. L., 1997, ApJS, 111, 377
Worthey G., 1997, in, Holt S. S., Mundy L. G., eds, Star Formation Near and Far, Vol. 393. Am. Inst. Phys. Press, Woodbury, NY, p. 525

This paper has been typeset from a TeX/LaTeX file prepared by the author.